

Current-voltage characteristic of narrow superconducting wires: Bifurcation phenomenaV. V. Baranov,¹ A. G. Balanov,² and V. V. Kabanov¹¹*Jozef Stefan Institute, Jamova 39, 1001 Ljubljana, Slovenia*²*Department of Physics, Loughborough University, Loughborough, United Kingdom*

(Received 21 April 2011; revised manuscript received 29 June 2011; published 26 September 2011)

The current-voltage characteristics of long and narrow superconducting channels are investigated using the time-dependent Ginzburg-Landau equations for the complex order parameter. We found out that the steps in the current-voltage characteristic can be associated with bifurcations of either a steady-state or oscillatory solution. We revealed typical instabilities which induced the singularities in current-voltage characteristics, and analytically estimated the period of oscillations and average voltage in the vicinity of the critical currents. Our results show that these bifurcations can substantially complicate dynamics of the order parameter and eventually lead to the appearance of such phenomena as multistability and chaos. The discussed bifurcation phenomena sheds a light on some recent experimental findings.

DOI: [10.1103/PhysRevB.84.094527](https://doi.org/10.1103/PhysRevB.84.094527)

PACS number(s): 74.40.Gh, 74.81.-g, 74.78.Na, 74.40.De

I. INTRODUCTION

The problem of the appearance of the resistive state in narrow superconducting channels when the current j exceeds the value of the critical current j_c was the subject of intensive debates in the past.¹ The voltage between two parts of the superconducting wire appears when the superconducting order parameter (OP) is strongly suppressed near the phase slip center (PSC). The phase of the OP becomes a very steep function across the PSC and finally demonstrates a 2π jump exactly when the OP reaches 0.^{1,2} This process appears periodically in time leading to the oscillation of the OP and nonlinear current-voltage characteristic (CVC) with well-pronounced steps of voltage when j reaches certain critical values.^{3,4}

The PSC has been extensively investigated theoretically and experimentally in the past (see Ref. 1 and references therein). It is well established that if $j > j_2 \sim j_c l_E^2 / \xi^2$ the normal state is absolutely stable; here l_E is the penetration depth of the electric field into the superconductor and ξ is the superconducting coherence length. Therefore if $l_E \gg \xi$ there is a wide interval of currents $j_c < j < j_2$ where the superconducting state coexists with the normal state leading to the oscillating type of behavior.^{5,6}

The steps in the CVC are usually interpreted as points where new PSC penetrates to the wire.^{1,3,4} It was also demonstrated that the time average of the voltage V and the frequency of oscillations ω satisfy the relation similar to the Josephson relation $V \propto \omega$.¹ The theoretical interpretation of the CVC is usually based on the static model of the resistive state^{3,7} or a very similar dynamical theory of the resistive state.^{1,8} All these models are based on the approximate time averaging of the time-dependent Ginzburg-Landau equations (TDGLEs) over a period. Therefore the complex behavior of the order parameter during one cycle is lost in these theories. An important step forward in the analysis of the TDGLEs has been made recently.^{9,10} It has been found that the dynamic of the order parameter in the PSC is governed by the ratio between the relaxation times of the TDGLEs.^{2,9,10} It has been established that the CVC exhibits an S shape in the regime of the fixed voltage. Besides, it has been shown that in the limit of the strong pair breaking effect due to interaction with phonons the

CVC demonstrates strong hysteresis in the regime of constant current.⁹ This behavior appears because two different solutions may coexist at the same value of the current. All these results (see also Refs. 11 and 12) demonstrate that different periodic and quasiperiodic in time solutions emerge with the changing of the voltage and current.¹³ However, some of the properties of these solutions are still not understood. In particular, the types of instabilities, as a result of which one solution is replaced by another one, are not identified. The theory still lacks an accurate analytical description of the CVC and well-defined and experimentally verifiable predictions. In this paper we present a detailed study of the CVC in the resistive state of superconductors with different lengths.

We reveal the types of instabilities (bifurcations) corresponding to the discontinuities on the CVC and derive an analytical expression for CVC when $j \rightarrow j_c$. We predict the appearance of the frequency in the spectrum of the electromagnetic radiation generated by the current after the period doubling bifurcation. This frequency equals exactly half of the one before the bifurcation point. Besides, we identify the positions of the PSCs in the wire and prove that our predictions on the basis of TDGLEs are in excellent agreement with the recent experimental results of Sivakov *et al.*¹⁴

Recent experimental studies have detected the spatial positions of PSCs in the different parts of the CVC.^{4,14} With the help of low-temperature laser scanning microscopy technique it was demonstrated that each quasilinear part of the CVC has a different number of the PSCs. When the current becomes larger than j_c the first PSC appears in the middle of the wire. Further increase of the current leads to the second step in voltage. Two PSCs appear symmetrically with respect to the center of the wire. Further increase of the current leads to the appearance of the third step in voltage and the third PSC is created in the center of the wire (see Fig. 2 of Ref. 14).

Another important effect was observed recently on the CVC of submicron BSCCO bridges.¹⁵ When the temperature of the bridge is reduced below T_c , characteristic steps on the CVC appear with clearly observed hysteresis. The measurement of the voltage as a function of time at high temperatures and at the fixed current has demonstrated sharp switching between two metastable states. The voltage randomly jumps between two values (random telegraph noise).¹⁵ The average

frequency of the switching is a very strong function of temperature: Decreasing of temperature by 1 K leads to the decrease of the frequency of switching by several orders of magnitude. Therefore the activation energy that corresponds to the switching is more than 10^4 K,¹⁵ indicating the macroscopic nature of the barrier between metastable states.

In our work, which involves numerical and analytical analysis of TDGLEs, we show that each step of the CVC is associated with transitions between different dynamical regimes, which are caused by the instabilities developed in the system. At $j = j_c$ the steady-state solution is changed by periodic oscillations (a limit cycle in the phase space), constituting the transition known in literature as the saddle-node homoclinic bifurcation.¹⁶ With the further increase of j this periodic oscillations eventually lose their stability, and new oscillations with doubled period occur in the system, thus evidencing the period-doubling bifurcation. These two transitions are universal and do not depend on the length L . On the contrary, the next bifurcation point is not universal and depends on L . With the further increase of L we observe the effect of multistability, when two or more different periodic regimes can be realized at the same value of the current. In this case, several limit cycles coexist in the phase space of the system, and realization of the particular regime depends on initial conditions.

II. MAIN EQUATIONS

The first TDGLE in dimensionless units has the form,

$$u \left(\frac{\partial \psi}{\partial t} + i\phi\psi \right) = \frac{\partial^2 \psi}{\partial x^2} + \psi - \psi|\psi|^2. \quad (1)$$

The second equation defines the stationary current through one-dimensional (1D) wire:

$$j = -\frac{\partial \phi}{\partial x} + \frac{1}{2i} \left(\psi^* \frac{\partial \psi}{\partial x} - \psi \frac{\partial \psi^*}{\partial x} \right). \quad (2)$$

Here ψ is the dimensionless complex OP, the distance is measured in units of the coherence length ξ and time is measured in units of the phase relaxation time $\tau_\theta = \frac{4\pi\lambda^2\sigma_n}{c^2}$, λ is the penetration depth, σ_n is the normal state conductivity, and c is the speed of light. The parameter $u = \frac{\tau_\psi}{\tau_\theta}$ is a material-dependent parameter, where τ_ψ is the relaxation time of the amplitude of the OP. The electrostatic potential ϕ is measured in the units of $\phi_0/2\pi c\tau_\theta$, where $\phi_0 = \pi\hbar c/e$ is the flux quantum, e is the electronic charge, and \hbar is the Planck constant; the dimensionless current density j is defined in the units of $\phi_0 c/8\pi^2\lambda^2\xi$. Nonequilibrium superconductors are characterized by an additional length scale l_E which describes the penetration of the electric field. From Eqs. (1) and (2) it follows that $l_E = \xi/u^{1/2}$. The time-dependent Ginzburg-Landau equations for the complex order parameter were derived for $T < T_c$ in the late 60th.^{17,18} The simplified version of the TDGLEs used in this work corresponds to the so-called gapless case with a large concentration of magnetic impurities $\tau_s T_c \ll 1$, where τ_s is the relaxation time on magnetic impurities.¹⁹ In that case parameter u is 12. More realistic generalized TDGLEs are derived in the dirty limit $\tau_{\text{im}} T_c \ll 1$, where τ_{im} is impurity scattering time. These equations take into account inelastic scattering by phonons.

In that case parameter u is 5.79. The penetration depth of the electric field l_E is substantially enhanced if the inelastic scattering time is large enough. The enhancement of l_E may be approximated in the case of gapless superconductivity if we assume that the phenomenological parameter u is small ($u < 1$).⁸ This approximation is widely accepted in the literature and leads to qualitatively and often quantitatively correct results above and below T_c . Note that the generalized TDGLEs have an additional time derivative term which may lead to different dynamics at $j > j_c$.¹⁹ However, as it is pointed out in Ref. 20 [Eq. (196) and Fig. 8, p. 499], the effect of this term becomes very small at large currents, while in the vicinity of the critical current the influence of this term has quantitative character without changing the qualitative behavior. The instability at $j = j_c$ is governed by the behavior of the Lyapunov exponents close to the instability point. Since the behavior of the Lyapunov exponents is similar for both types of equations we believe that the dynamics described by both equations are qualitatively the same in the whole region of currents $j > j_c$. Therefore, Eqs. (1) and (2) should describe qualitatively well the gapless superconductors with large concentrations of magnetic impurities as well as ordinary superconductors in the dirty limit ($\tau_{\text{im}} T_c \ll 1$). Since most of our results are qualitative we believe that they are quite general and applicable to many experimental cases.

Here we consider the superconducting wire of a length L with the following boundary conditions: $\rho(-L/2) = \rho(L/2) = 1$ and $d\phi(-L/2)/dx = d\phi(L/2)/dx = 0$, where we define phase θ and modulus ρ of the order parameter according to the relation $\psi = \rho \exp(i\theta)$. The absence of the electric field at the end of the wire determines the gradient of phase $d\theta(-L/2)/dx = d\theta(L/2)/dx = j$.

III. RESULTS AND DISCUSSIONS

We start with the analysis of the steady-state solutions of the TDGLEs (1) and (2), which are defined as $\psi = (1 - k^2)^{1/2} \exp(ikx)$. The equation for k has the form $j = (1 - k^2)k$, and for $j < j_c = 2/3\sqrt{3}$ it yields two roots $k_1 < k_2$. The first solution corresponding to k_1 is stable and the second (k_2) is unstable.

When the current reaches its critical value $j = j_c$ these steady-state solutions collide with each other ($k_1 = k_2$) and disappear, thus suggesting a saddle-node bifurcation. Indeed, the stability analysis of the steady-state solution performed in Ref. 2 shows that only one Lyapunov exponent crosses 0 when $j = j_c$. Additionally, our numerical calculation revealed that at the moment of this bifurcation, a periodic solution (limit cycle) with a very large period arises in the phase space of the system in the very close vicinity of the disappeared steady states. As j grows, the period of the limit cycle quickly decreases. All those facts evidence that at $j = j_c$ the systems undergo the saddle-node homoclinic bifurcation.¹⁶

Note that the value of $j_c = 2/3\sqrt{3}$ is obtained for the wire of the infinite length. The boundary conditions for Eqs. (1) and (2) defined above lead to the slightly different value of the critical current. Therefore the value of $j_c(L)$ should be determined from the solution of stationary equations [Eqs. (1) and (2)] with the same boundary conditions.

According to the theory of dynamical systems, the behavior of a system in the vicinity of the saddle-node homoclinic bifurcation can be described by the normal form,¹⁶

$$\dot{y} = \beta + a(0)y^2, \quad (3)$$

where y is a representative phase variable, $\beta = -2^{3/2}u(j - j_c)/3(u + 2)j_c$, and $a(0) = -2^{3/2}u/(u + 2)$. To derive the normal form we have to follow the standard recipe.¹⁶ It is convenient to rewrite the TDGLEs (1) and (2) in the limit of $L \rightarrow \infty$ in terms of ρ and the gauge invariant scalar $\Phi = \phi + \partial\theta/\partial t$ and vector $Q = \partial\theta/\partial x$ potentials.

$$\begin{aligned} u\partial\rho/\partial t &= \partial^2\rho/\partial x^2 + \rho(1 - \rho^2 - Q^2), \\ u\rho^2\Phi &= \partial(\rho^2Q)/\partial x, \\ j &= -\partial\Phi/\partial x + \partial Q/\partial t + \rho^2Q. \end{aligned} \quad (4)$$

These equations have the steady-state solution $\rho = \rho_0 = \sqrt{2/3}$, $\Phi = 0$, $Q = 1/\sqrt{3}$, $j = j_c$, which becomes unstable and has one Lyapunov exponent λ_0 which crosses 0 at $j = j_c$. Expanding Eq. (4) up to the second order in deviations from the steady-state solution, rescaling the time $t/u \rightarrow t$ and projecting this equation on the direction of the eigenvector corresponding to λ_0 we obtain Eq. (3). The normal form (3) allows one to predict the period T of the periodic solution which corresponds to the limit cycle. Following to Eqs. (32) and (23) of Ref. 21 we integrate Eq. (3) over y between $\pm y_1$ where y_1 is of the order of 1. $T = 2 \tan^{-1}(y_1 \sqrt{a(0)/\beta})/\sqrt{a(0)\beta}$. Therefore, when $(j - j_c)/j_c \ll 1$ the period of oscillations is determined by the formula:

$$T = \pi/\sqrt{a(0)\beta} = \frac{\pi\sqrt{3}(u + 2)}{2^{3/2}u} [(j - j_c)/j_c]^{-1/2}. \quad (5)$$

To verify theoretical prediction we have performed extensive numerical simulations of Eqs. (1) and (2), using the fourth-order Runge-Kutta method. The spatial derivatives are evaluated using a finite difference scheme of the second and fourth order. The calculations were performed for the superconducting wire of three different length $L = L_0$, $2L_0$, and $4L_0$ ($L_0/\xi = 10.88$) and for $u = 1/2$. The different length leads to a slightly different value of the critical current caused by the boundary conditions. The calculated critical currents are $j_c(L)/j_c = 1.016$, 1.002 , and 1.00019 , respectively. Some properties of the solution are universal and do not depend on the length L . On the other hand, there are some features of the solution and the CVC which are not universal and depend on the length L .

The first universal property of the solution is the dependence of the period of the oscillation on $(j - j_c(L))/j_c(L)$ in the range of currents $j_c(L) < j < j_{c1}(L)$, where $j_{c1}(L)$ is the first critical current where the limit cycle loses its stability. According to Eq. (5) $T \approx 9.62[(j - j_c(L))/j_c(L)]^{-1/2}$ for $u = 1/2$. The results of calculations of the period for the oscillatory solution are plotted in Fig. 1 for all three lengths L together with the analytical estimate, given by Eq.(5). There is very good agreement of numerical results with Eq.(5) over more than four orders of magnitude in $(j - j_c(L))/j_c(L)$. Since Eq. (5) describes the asymptotic behavior of the period T in the limit $(j - j_c(L))/j_c(L) \rightarrow 0$ the agreement becomes better when the current is closer to its critical value.

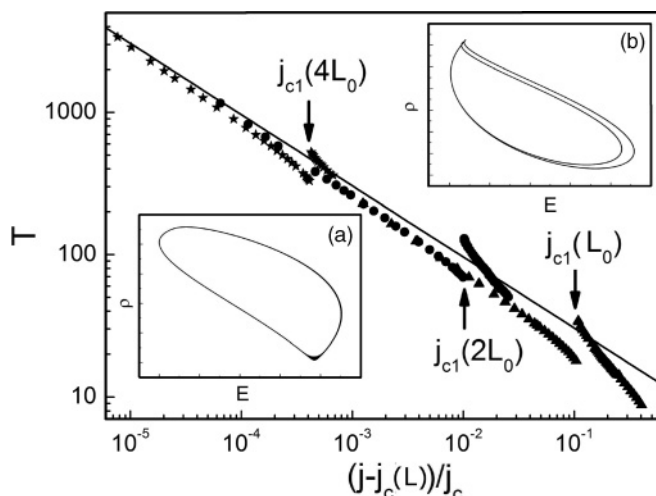


FIG. 1. The period of the solution as a function of current for three different lengths of the wire: $L = L_0$ (triangles), $2L_0$ (circles), $4L_0$ (stars). The solid line represents the results of Eq. (5). Arrows indicate the period-doubling bifurcation point $j_{c1}(L)$. Insets represent projection of the limit cycle trajectory to the $[\rho(0), E(0)]$ plane before (a) and after (b) bifurcation point $j_{c1}(L)$. Here $E(0)$ is the electric field in the center of the wire.

The divergence of the period implies that the CVC near $j_c(L)$ should have the nonlinear form $V \propto T^{-1} \propto [(j - j_c(L))/j_c(L)]^{1/2}$ (Fig. 2). This type of dependence is due to the quantization rule, derived in Ref. 22, that connects the averaged electric field and the period of oscillations. Indeed, as it is clearly seen from Fig. 2, the voltage V shows the universal dependence in accordance with Eq. (5). Note that similar CVCs have been reported earlier.⁹ However, the authors did not recognize the type of bifurcation and did not derive the normal form for this bifurcation. As a result they were unable

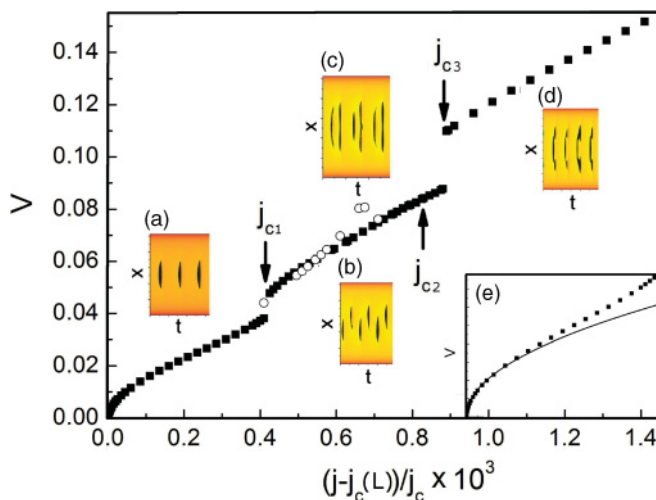


FIG. 2. (Color online) The CVC of the channel with $L = 4L_0$. Open circles represent the more complex limit cycles, which coexist with the main periodic solution (multistability). Insets (a)–(d) show the space-time arrangements of the PSCs in different regions of the CVC. The inset (c) corresponds to open circles. Inset (e) shows the CVC for $j < j_{c1}(L)$ in comparison with the analytical formula (see the text).

to get an analytical expression for CVC in the vicinity of j_c . An accurate solution of dynamical Eqs. (1) and (2) and asymptotic, predicted by Eq. (5), does not confirm an approximate result $V \propto -1/\ln((j - j_c)/j_c)$, derived in Ref. 1. The square root behavior of the CVC, however, is in agreement with the earlier result of Aslamazov and Larkin,²³ who had considered the CVC of the short ($L \ll \xi$) superconducting bridge.

For relatively small currents $j_c(L) < j < j_{c1}(L)$ the phase slip center appears periodically in time in the center of the wire (Fig. 2) in the agreement with the experimental results.¹⁴ This oscillating behavior of the OP leads to the oscillating behavior of the voltage and emission of an electromagnetic radiation with the frequency $\omega_1 \propto T^{-1}$.

Further increase of the current leads to instability of the limit cycle. At $j = j_{c1}(L)$ the periodic solution becomes unstable and a new limit cycle emerges as the result of period-doubling bifurcation. This is clearly seen from Fig. 1 where a sudden increase of the period is observed at $j = j_{c1}(L)$. It appears that this instability is universal and does not depend on the length L .

The period-doubling bifurcation could be easily recognized if we plot the cycle trajectories below and above $j_{c1}(L)$. It is important to plot trajectories only for the gauge invariant quantities to avoid unphysical effects. Therefore, in the insets to Fig. 1 we present the periodic solution in coordinates $\rho(x=0)$ and electric field $E(x=0) = -d\phi(x=0)/dx$. As clearly seen from this figure, the period-doubling bifurcation manifests itself in the transition from a single-loop (period-1) limit cycle to a double-loop (period-2) limit cycle.²⁴

This bifurcation also leads to the singular behavior of the CVC. This singularity is more prominent for longer wires $L = 4L_0$ where the jump of voltage is well pronounced, while for $L = L_0$ it manifests itself only by the change of the slope [Fig. 3(a)]. The arrangement of the PSCs in space and time is plotted in Fig. 2. As it follows from Fig. 2, at $j = j_{c1}(L)$ the position of one PSC is shifted up with respect to the center and the position of the next PSC is shifted down. Therefore, the period of a new limit cycle is twice the period of the limit cycle before the bifurcation point. Each period includes now two PSCs; one is slightly above and another is slightly below the center of the wire, which is well agreed with experimental observations.¹⁴ As a result of period doubling, a new frequency $\omega_2 = \omega_1/2$ appears in the spectrum of the electromagnetic radiation generated by the current. It should be pointed out that the period-doubling bifurcation in the superconducting channel with fixed voltage was reported earlier.¹³ Nevertheless there is substantial geometric difference between these two cases. In Ref. 13 the PSCs were always detected in the center of the wire, in contrast with our results.

Note that the critical current for period-doubling bifurcation $j_{c1}(L)$ is not universal and strongly depends on the length of the channel L . According to Fig. 3 ($j_{c1}(L) - j_c$)/ $j_c = 0.125, 0.012, 0.0006$ for $L = L_0, 2L_0$, and $4L_0$, respectively. Indeed it demonstrates the exponential dependence on the length L , as it was proposed in Ref. 25.

The next bifurcation which is common for all studied cases is the destruction of the periodic cycle. For all studied cases there exists the second critical current $j_{c2}(L)/j_c = 1.44, 1.027$, and 1.001 for $L = L_0, 2L_0$, and $4L_0$, respectively, where the

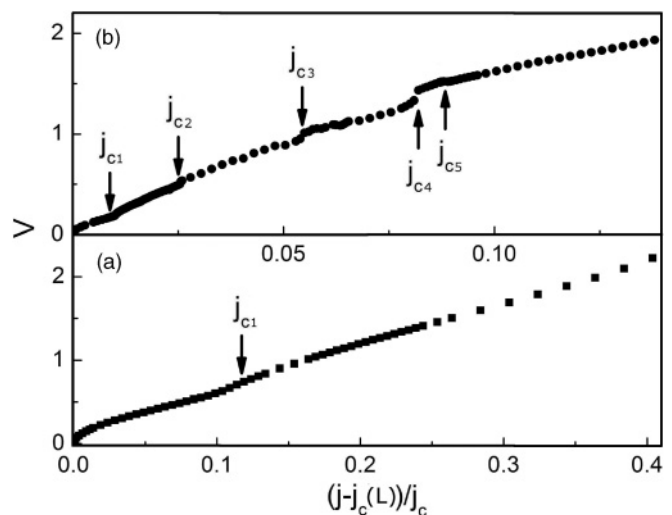


FIG. 3. The CVC of the wire (a) $L = L_0$ and (b) $L = 2L_0$. Arrows indicate different bifurcation points.

periodic solution loses its stability. This transition does not show any clear singularity on the CVC. In all studied cases instead of the periodic solution we have found an oscillating, but nonperiodic, solution. The Fourier transform of the voltage contains broad features instead of the δ function like spectrum before the transition. The solution in the vicinity of $j_{c2}(L)$ is characterized by long intervals of time where the solution is almost periodic and topologically similar to the solution before the bifurcation point $j < j_{c2}(L)$. Then the instability develops and the solution moves far away from the periodic cycle. After few periods the solution is coming back again to a very similar oscillating trajectory and performs regular oscillations for many periods. To demonstrate this behavior we calculate a Poincaré map for $j_{c2} < j < j_{c5}$ and $L = 2L_0$. The projection of the phase trajectory to the plane $[\rho(-L/4), E(-L/4)]$ never crosses the space near the center of the trajectory. Therefore we chose the Poincaré section as a plane which crosses the center of this trajectory $E(-L/4) = 0.04$ for $j/j_c = 1.0278$. In Fig. 4 we plot the projection of the Poincaré map to $\rho(0)$ and

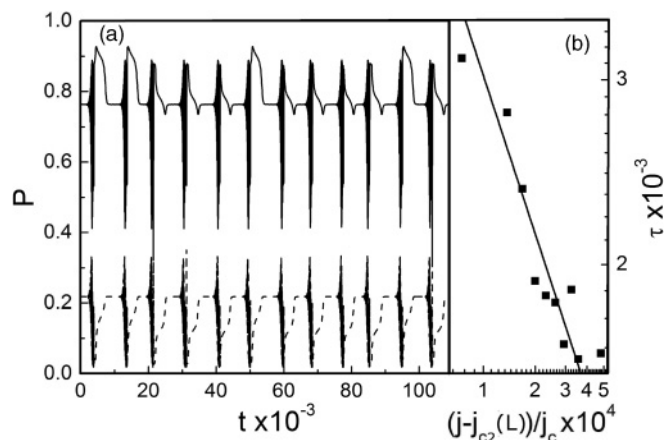


FIG. 4. (a) The projection of the Poincaré map on $\rho(0)$ (solid line) and $E(0)$ (dashed line) as a function of time. (b) The averaged period of the laminar phase as a function of current (squares). The solid line shows analytical prediction (see the text).

$E(0)$ as a function of discrete time, when trajectory crosses the Poincaré section. The long horizontal lines represent an almost periodic solution. The time during which solution stays near the periodic laminar orbit becomes larger and larger when $j \rightarrow j_{c2}(L) + 0$, as demonstrated in the inset of Fig. 4.^{21,24} According to Eqs. (32) and (23) of Ref. 21 the time that the trajectory stays near the regular limit cycle is proportional to $\tau \propto (j - j_{c2}(L))^{-1/2}$. The inset in Fig. 4 demonstrates that τ indeed increases as $(j - j_{c2}(L))^{-1/2}$ indicating that we deal with chaotic solution which is developing via the intermittence.²⁴

Further increase of the current for the case of $L = 2L_0$ leads to an additional step of voltage [$j_{c3}(L)/j_c = 1.058$] in the CVC. In that case two remote PSCs located symmetrically with respect to the center of the channel are accompanied by the third one, which appears in the middle of the wire [Fig. 2(d)]. This does not destroy chaos, although it changes apparently its topological properties. The CVC in this region of currents has some nonregular behavior [Fig. 3(b)], which might be associated with the appearance and disappearance of the so-called “periodic windows,” areas of the parameter values, where limit cycles with a relatively large period become stable.²⁴

The next step in voltage at $j_{c4}(L)/j_c = 1.084$ is associated with the creation of a new PSC, again without the change of the chaotic character of the solution. And finally, the nonperiodic orbit disappears and a limit cycle becomes stable in the relatively large window of currents [$j_{c5}(L)/j_c = 1.098 < j/j_c < 1.114$]. This bifurcation produces a voltage step on the CVC, and in contrast to all previous cases, the voltage decreases at the bifurcation point [Fig. 3(b)]. The corresponding limit cycle has four PSCs, each of which has different positions in the channel. Remarkably, such behavior of the PSC was previously observed in experiments.¹⁴

The situation for the longer channel $L = 4L_0$ is slightly different. First, we have found that for $j > j_{c1}(L)$ there are few ranges of the current where other limit cycles coexist with the main periodic solution, similarly to the earlier report.⁹ Therefore, at the same value of the current we observe different stable periodic solutions with their own attracting phase spaces. The multistability is found only in the case of the long channel ($L = 4L_0$). In the case of $L = L_0$ and $2L_0$ we were unable to find any manifestation of multistability. The region where chaos is developed via the intermittence for the long channel $L = 4L_0$ is much more narrow than in the case of $L = 2L_0$. The chaotic oscillations become very quickly unstable and a new stable limit cycle with three PSCs

appears at $j/j_c > j_{c3}(L)/j_c = 1.0011$ in contrast with the former case, where this solution has also an irregular chaotic behavior. This bifurcation manifests itself by the step in voltage on the CVC and is consistent with the observation made in Ref. 14.

The effect of multistability revealed in our calculations may be related to the effects of switching between two metastable states, discussed in Ref. 15. Indeed the existence of two different limit cycles with the different topology of phase trajectories and different averaged voltage implies that relatively large thermodynamic fluctuations may switch from one trajectory to another. If the switching is fast and the averaged time between switchings is large in comparison with the period of the limit cycle, the measured voltage will be averaged over many periods. The switching requires overcoming the energy barrier between two limit cycles therefore the time between two switchings is an exponential function of temperature. In the case of wide bridges the activation energy is macroscopic and depends on the width of the sample. Therefore, in the case when the time of measurements is larger than the period of the cycle and shorter than the average time between the switchings, the fluctuations of the voltage look like a telegraph noise and are similar to that observed in Ref. 15.

IV. CONCLUSIONS

In conclusion, we have analyzed the current-voltage characteristics of the superconducting channel of a different length. We have proven that the steady-state solution loses its stability as a result of the saddle-node homoclinic bifurcation, which leads to a limit cycle of the diverging period. This unambiguously leads to the singular $V \propto (j - j_c)^{1/2}$ CVC. We have demonstrated that the second anomaly in the CVC is caused by the period-doubling bifurcation. The main consequence of this bifurcation is the appearance of the new frequency in the spectrum of electromagnetic radiation which equals exactly half of the frequency before bifurcation. The appearance of the third PSC is not universal. In short channels this bifurcation appears when the solution has chaotic character. Increasing the channel’s length L stabilizes a periodic solution with three PSCs. In the intermediate range of currents the periodic solution becomes unstable leading to the chaos, which is developed via the intermittence. The effect of multistability in the presence of thermodynamic fluctuations may be responsible for the switching between two periodic solutions and random jumps of voltage between two averaged values.

¹B. I. Ivlev and N. B. Kopnin, *Usp. Fiz. Nauk.* **142**, 435 (1984) [*Sov. Phys. Usp.* **27**, 206 (1984)].

²M. Lu-Dac and V. V. Kabanov, *Phys. Rev. B* **79**, 184521 (2009); *J. Phys. Conf. Ser.* **129**, 012050 (2008).

³W. J. Skocpol, M. R. Beasley, and M. Tinkham, *J. Low Temp. Phys.* **16**, 145 (1974).

⁴I. M. Dmitrenko, *Fiz. Nizk. Temp.* **22**, 849 (1996) [*Low Temp. Phys.* **22**, 648 (1996)].

⁵L. Kramer and R. J. Watts-Tobin, *Phys. Rev. Lett.* **40**, 1041 (1978).

⁶L. Kramer and A. Baratoff, *Phys. Rev. Lett.* **38**, 518 (1977).

⁷V. P. Galaiko, *Zh. Eksp. Teor. Fiz.* **66**, 379 (1974) [*Sov. Phys. JETP* **39**, 181 (1974)].

⁸B. I. Ivlev, N. B. Kopnin, and L. A. Maslova, *Zh. Eksp. Teor. Fiz.* **78**, 1963 (1980) [*Sov. Phys. JETP* **51**, 986 (1980)]; B. I. Ivlev, N. B. Kopnin, and I. A. Larkin, *ZhETF* **88**, 575 (1985) [*Sov. Phys. JETP* **61**, 337 (1985)].

- ⁹S. Michotte, S. Mátéfi-Tempfli, L. Piraux, D. Y. Vodolazov, and F. M. Peeters, *Phys. Rev. B* **69**, 094512 (2004).
- ¹⁰D. Y. Vodolazov and F. M. Peeters, *Phys. Rev. B* **66**, 054537 (2002).
- ¹¹G. R. Berdiyrov, M. V. Milosević, and F. M. Peeters, *Phys. Rev. B* **80**, 214509 (2009).
- ¹²G. R. Berdiyrov, A. K. Elmurodov, F. M. Peeters, and D. Y. Vodolazov, *Phys. Rev. B* **79**, 174506 (2009).
- ¹³J. Kim, J. Rubinstein, and P. Sternberg, *Physica C* **470**, 630 (2010).
- ¹⁴A. G. Sivakov, A. M. Glukhov, A. N. Omelyanchouk, Y. Koval, P. Muller, and A. V. Ustinov, *Phys. Rev. Lett.* **91**, 267001 (2003).
- ¹⁵S. V. Zybtshev, V. Ya. Pokrovskii, I. G. Gorlova, Yu. I. Latyshev, V. V. Luchinin, and A. Yu. Savenko, *J. Low Temp. Phys.* **139**, 351 (2005); S. V. Zybtshev, V. Ya. Pokrovskii, I. G. Gorlova, Yu. I. Latyshev, V. V. Luchinin, A. Ya. Savenko, and V. N. Timofeev, *ibid.* **139**, 3511 (2005); S. V. Zybtshev, V. Ya. Pokrovskii, I. G. Gorlova, Yu. I. Latyshev, and V. N. Timofeev, *J. Phys. Conf. Ser.*, **43**, 643 (2006).
- ¹⁶Yu. A. Kuznetsov, *Elements of Applied Bifurcation Theory, Applied Mathematical Science*, Vol. 112 (Springer-Verlag, New York, 2004).
- ¹⁷L. P. Gorkov and G. M. Eliashberg, *ZhETF* **54**, 612 (1968) [*Sov. Phys. JETP* **27**, 328 (1968)].
- ¹⁸E. Abrahams and T. Tsuneto, *Phys. Rev.* **152**, 416 (1966).
- ¹⁹N. B. Kopnin, *Theory of Nonequilibrium Superconductivity* (Clarendon Press, Oxford, 2001).
- ²⁰R. J. Watts-Tobin, Y. Krahenbuhl, and L. Kramer, *J. Low Temp. Phys.* **42**, 459 (1981).
- ²¹L. D. Landau and E. M. Lifshitz, *Hydrodynamics* (Nauka, Moscow, 1988).
- ²²B. I. Ivlev and N. B. Kopnin, *Pis'ma ZhETF* **28**, 640 (1978) [*Sov. Phys. JETP Lett.* **28**, 592 (1978)].
- ²³L. G. Aslamazov and A. I. Larkin, *Pis'ma ZhETF* **9**, 150 (1969) [*Sov. Phys. JETP Lett.* **9**, 87 (1969)].
- ²⁴V. S. Anishchenko, *Dynamical Chaos—Models and Experiments. Appearance Routes and Structure of Chaos in Simple Dynamical Systems* (World Scientific Publishing, Singapore, 1995).
- ²⁵V. P. Galaiko, *ZhETF* **68**, 223 (1975) [*Sov. Phys. JETP* **41**, 108 (1975)].